Sensors & Actuators: B. Chemical 282 (2019) 391–398

Contents lists available at ScienceDirect

Sensors and Actuators B: Chemical

journal homepage: www.elsevier.com/locate/snb

$LiNbO_3$ integrated system for opto-microfluidic sensing

G. Bettella[a], R. Zamboni[a], G. Pozza[a], A. Zaltron[a], C. Montevecchi[a], M. Pierno[a], G. Mistura[a], C. Sada[a,*], L. Gauthier-Manuel[b], M. Chauvet[b]

[a] Physics and Astronomy Department, University of Padova, Via Marzolo 8, 35131 Padova, Italy
[b] FEMTO-ST Institute, UMR 6174, University of Bourgogne Franche-Comté, 15B Avenue des Montboucons, 25000 Besançon, France

ARTICLE INFO

Keywords:
Microfluidic
Droplet
Optical trigger
Waveguide
Lithium niobate
Lab-on-a-Chip

ABSTRACT

In this work, we realized and tested an integrated opto-microfluidics platform entirely made on lithium niobate ($LiNbO_3$) crystals, able to detect the single droplet passage and estimate its size without the need of any imaging processing. It is based on the coupling of a self-aligned integrated optical stage, made of an array of optical waveguides, to a microfluidic circuit such as a T-junction or Cross-junction engraved in the same substrate. The platform presented high quality performances in terms of optical triggering, reproducibility and stability in time, allowing in real-time data analysis. The comparison with standard approaches using microscopes and fast camera imagining acquisition and relative post-processing, showed an increased capability better than 50%. The demonstrated feasibility of integration of these two stages will allow the realization of a Lab-On-a-Chip on a monolithic substrate of lithium niobate, exploiting its multiple applications for manipulation of droplets.

1. Introduction

Since the development of devices for inkjet printer in the '50s, microfluidic technology has been addressed as a highly performant and reliable tool for a wide range of applications, such as chemical and biological analysis and sensing [1]. Although the microfluidics devices are compact and have a reduced size, in most of the cases they still require bulky and extra optical set-ups to investigate and detect the fluid and dispersed phases within, such as microscopes and imaging processes. In particular, fast sensing applications typically require expensive fast cameras, large data storage and need long post processing analysis, which make unfeasible a real-time sensing. This lack of integration and portability between the microfluidic device and the optical detection set-up is one of the main issue for non-massive commercialization of microfluidic devices, thus keeping most of the prototypes just at a proof-of-concept. For these reasons, increasing attempts to integrate multiple stages on the same substrate have been proposed. Among others, the realization of an optical stage, able to detect and identify the flow of objects inside micro-channels has particular interest especially in the field of particle sensing and actuation. Many solutions have been tested to substitute imaging techniques: the embedding of optical fibers in polymeric based device [2–5], the integration of waveguide by means of micro-lenses to focus the light in the middle of the fluidic channels [6], the integration of localized LED sources [7,8] or photodiodes [8,9], and capacitive sensing [10–15] or thermal sensing [16] by means of electrode are the most investigated. However, each of them has severe drawbacks: for example, electrodes exhibit degradation problems and may be too invasive; while the fiber coupling and the combination of waveguide with lenses suffer for very low reproducibility in the fabrication, like aligning problems. Some tests have been tried to integrate a waveguide with a microfluidic channel [17–19], but in channels roughness did not allow a perfect coupling, maintaining align problem.

Recently, lithium niobate ($LiNbO_3$) has been proposed as a valid alternative for integrating [20–22] multiple stages on the same substrate, thanks to its numerous properties already exploited in integrated optics. Although this material is widely exploited for electro-optical devices and for realizing optical systems, such as second harmonic generators [23], optical modulators and waveguides [24,25], in the last years it has been demonstrated also to be an interesting material for microfluidic applications. As a matter of fact, it has been already exploited as active substrate for acoustic wave generation [26] and particle trapping [27–30] in liquids, as well as light-controlled switcher of liquid crystal [31]. Furthermore, only recently the feasibility of

* Corresponding author.
E-mail addresses: giacomobettella@gmail.com (G. Bettella), riccardo.zamboni@phd.unipd.it (R. Zamboni), gianluca.pozza@gmail.com (G. Pozza), annamaria.zaltron@unipd.it (A. Zaltron), carlo.montevecchi@gmail.com (C. Montevecchi), matteo.pierno@unipd.it (M. Pierno), giampaolo.mistura@unipd.it (G. Mistura), cinzia.sada@unipd.it (C. Sada), ludovic.gauthier-manuel@univ-fcomte.fr (L. Gauthier-Manuel), mathieu.chauvet@univ-fcomte.fr (M. Chauvet).

https://doi.org/10.1016/j.snb.2018.10.082
Received 18 April 2018; Received in revised form 1 October 2018; Accepted 15 October 2018
Available online 02 November 2018

microchannels fabrication in lithium niobate by means of dicing [22,32], laser ablation [22,33,34], micromilling [35], and even for droplet generation circuits [20,22] has been proven. These features make this material an optimal candidate for Lab-On-a-Chip (LOC) applications.

In this work, we present the first self-aligned opto-microfluidic platform completely integrated in lithium niobate for optical detection of dispersed phases in fluids, such as droplets, by coupling a cross-shape junction for droplets generation and optical waveguides array all realized on the same substrate. As a matter of fact, the generation and detection of droplets are the first main steps for the subsequent realization of a more complex multifunctional LOC.

Both the fluidic and optical stages were realized on the same commercial lithium niobate crystal. Microfluidic channels were engraved by exploiting a precision saw with a polymeric blade, as recently discussed in [22], crossing orthogonally an array of optical waveguides previously realized via titanium in-diffusion. In this way, the waveguides can be exploited to illuminate fluids and objects present in the channels and, at the same time, to detect the transmitted or emitted light. As demonstrated by Bettella et al. [22], the micromachining process used for the realization of the fluidic circuit provides the low roughness for the lateral walls of the channels, so that the transmission of the optical waveguides is not perturbed by light diffusion at the interfaces. It significantly simplifies the fabrication since no further chemical or mechanical treatment of surfaces is necessary. Moreover, the fabrication of the waveguide in a single step require no mechanical alignment with the fluidic channel (as will be explained in the Experimental section), avoiding the irreproducibility in the aligning process between two optical stages on the two side of the microchannel.

Indeed, the $LiNbO_3$-based platform herein presented actuates as a self-aligned optical sensor sensitive to the passage of a single droplet, which is therefore analyzed individually so that its position, sizes, geometry and their optical properties can be monitored in real-time. Although we tested the device with droplets, the optical trigger concept can be extended to flowing objects of different nature, such as biological samples or particles. As a matter of fact, the high confinement of light provided by the integrated optical waveguides system not only allows the detection of objects at the micro-scale, but it is also highly sensitive to small difference of the refractive index.

2. Experimental

2.1. Chip fabrication

The opto-fluidic device consists in a monolithic substrate of lithium niobate, where a cross-shape droplet generator was engraved and coupled with an array of optical waveguides transverse to the main fluidic channel, as sketched in Fig. 1a. Z-propagating optical waveguides were realized on a 1 mm thick commercial congruent $LiNbO_3$ wafer (Crystal Technology) by titanium (Ti) local doping via thermal in-diffusion. The titanium doping was achieved by combining photolithographic and thin-film deposition techniques, as already described by the authors in [21].

A photoresist layer S1813 (S1800 series, Microchem) was spinned at the surface of the lithium niobate substrate (1 min at 6000 rpm) previously cleaned by plasma Oxygen and coated with primer based on hexathyldisilizane (HDMS) to enhance photoresist adhesion. A pattern constituted of 5 µm width stripes was then photo-induced by exposing the substrate to a UV illumination at 9 mW/cm^2 for 18 s, through a chrome mask fabricated on lime glass (Deltamask). Afterwards, the pattern was developed by dipping in a stirred bath of Microposit Developer MF-300 for 1 min and rinsed in distilled water. A 40 nm Ti thin film was then deposited at the patterned surface of the $LiNbO_3$ substrate via sputtering technique (sputtering conditions: Argon atmosphere at a pressure of 5×10^{-3} mbar and a deposition power of 40 W for 22 min). The titanium excess and photoresist were removed in a bath of SVC™-14 at 60 °C under sonication for few seconds, thus obtaining an array of 5 µm width titanium stripes equally spaced 2 mm apart. As a final step, a thermal treatment was performed in a tubular furnace (Hochtemperaturofen GmbH, model F-VS 100-500/13, Gero) at 1030 °C for 2 h in an oxygen atmosphere, thus promoting the complete Ti in-diffusion.

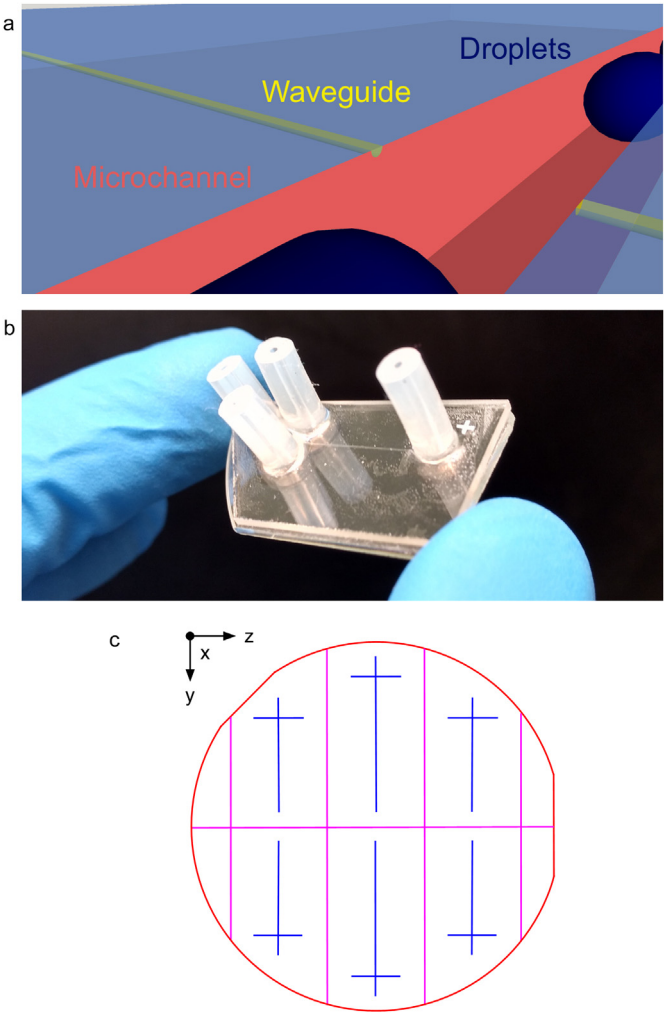

Fig. 1. Sketches of the lithium niobate chip: (a) device near the lateral wall of the channel, where waveguides output meet the microfluidic channel: in yellow the waveguides are represented facing each others cross the microchannel in red, in light blue lithium niobate substrate and in dark blue the flowing droplets. b) photo of the final device with lithium niobate on the bottom, glass cover on the top with tubings connections. c) Scheme of the cuts performed by the Disco saw 321, where red lines are the lithium niobate x-cut 3in wafer, magenta ones are the 1 mm deep cuts and the blue ones represent the microfluidic channels. (For interpretation of the references to colour in this figure legend, the reader is referred to the web version of this article.)

The resulting Titanium in-depth profile was determined by means of Secondary Ion Mass Spectrometry (SIMS) as reported in [21]. The doped layer is confined in few micrometers nearby the surface, presenting a semi-Gaussian profile with a half width at half maximum (HWHM) of (1.33 ± 0.06) µm. This configuration is needed to support a single optical mode propagation within the waveguide, but guaranteeing a section that covers 2% of the microfluidic channel height. Subsequently, the channel waveguides realized were characterized as in [22] showing a refractive index increase Δn_e at the surface equal to $1.12 \pm 0.03 \times 10^{-2}$ for extraordinary light and $\Delta n_o = (0.66 \pm 0.02) \times 10^{-2}$ for ordinary light.

This treated wafer was cut into six samples of 2 × 3 cm, as reported

in Fig. 1b (magenta lines) obtaining 6 different chips from one wafer. The cuts were performed by means of a Disco Dad 321 precision saw equipped with a diamond particle-polymeric blade. The same saw was exploited for engraving the microfluidic channels (blue lines in Fig. 1b), which are 200 µm wide and 100 µm deep. As already reported by the authors in [22], the lateral walls of the engraved circuit showed a good optical quality with lateral surface roughness of about 4 nm RMS, thus ensuring an optimum coupling of the waveguides with the microfluidic channels without the need for further chemical or mechanical treatments of the device. In particular, with this preparation protocol the waveguides result to be located at the top of the channel: this configuration presents the advantage to minimize and simplify the manufacturing steps respect the realization of waveguides centered respect the channel by way of Ti thermal diffusion. As a matter of fact, each waveguide is crossed and therefore interrupted by the engraved microfluidic channel: the net result is two identical waveguides perpendicular to the channel and faces each other and therefore perfectly aligned. One will play the role of input waveguide, the other that of output waveguide. This protocol is fully compatible with other integrated optical stages that can be realized on the lithium niobate surface such as optical modulators [36]. It also allows the study of the local interaction between an object (i.e. a droplet) and the surfaces of the channel, as needed in the case of laminar boundary layer or particle manipulation via dielectrophoretic/electrophoretic effects. Since the position of the waveguide respect to the channel is related to the trigger response of the device and, consequently, it allows to derive different information on the investigated objects. In the case of droplets, for instance, its length and the meniscus shape can be detected and monitored as well as the confinement due to the surface. In our case, the illuminated depth inside the channel is about 15–20 µm (15–20% of the channel height) since the waveguides is located at the top of the fluidic channel and has a numerical aperture of 0.22. Although a waveguide at the center of the microfluidic channel investigates a larger section of the channel, it is instead less sensitive to interfaces and requires many other manufacturing steps. In general an embedded waveguide is not normally compatible with optical stages realized on the surface of the material, thus limiting the LOC complexity of the integrated functionalities therein achievable.

Finally, the $LiNbO_3$ samples were sealed with a silica cover, with proper holes and silicon tubes for microfluidic inlets, as reported in Fig. 1b. The sealing procedure was achieved with the technique described by Langelier et al. [37] using a thin layer of NOA68® (Nordland Optics), an UV curable adhesive. Although lithium niobate has a hydrophobic behavior in all three different crystal directions [38] a 100 µM octadecyltrichlorosilane (OTS) solution in toluene was fluxed through the channels, in order to homogenize the microfluidic channels' hydrophobicity and increase the droplets production efficiency.

2.2. Optical trigger setup

The performances of the final device were characterized by means of the setup shown in Fig. 2. A He–Ne laser (wavelength = 632.28 nm, power = 4 mW) was coupled into one waveguide of the device by mean of a 20×/0.4 objective. The light polarization and power is controlled by a half wave plate (λ/2 in Fig. 2) and a polarizer (pol. in Fig. 2). The alignment between the beam and the waveguide was achieved by a 6 degree of freedom micropositioner. The chip holder allowed the fluidic connection with two independent syringe pumps (PHD 2000, Harvard Apparatus). The flows were controlled in order to produce MilliQ® droplets in a continuous phase of mineral oil (Sigma Aldrich) with 0.09% (w/w) surfactant SPAN80® (Sigma Aldrich). Thanks to the three inlets, the cross shape geometry allows the production of droplets in two possible configurations. The flow-focusing configuration, where the continuous phase is flowed in two orthogonal channels with respect to the dispersed phase, or the T-junction configuration where one of the three inlets is closed and the other two are used for flowing the two phases. Since the working principle of the optical microfluidic device is independent of the droplets production configuration, in this work tests and measurements were performed in the T-junction configuration. Indeed, the droplets flow in the same main channel coupled with the waveguides, irrespective of the generation process.

When passing in front of a waveguide, the droplets interact with the light from the input waveguide, and the output waveguide collects the transmitted light across the microfluidic channel. At the end of the output waveguide, the intensity was analyzed by a near field technique, using a Vidicon tube. The output was magnified up to 430 times, read by a silicon photodiode and amplified by mean of a transimpedance amplifier. Finally, the analog signal was digitalized through an oscilloscope Agilent MSO-X 2012A oscilloscope.

The setup was tested with different droplet lengths and frequency. The continuous phase flow Q_c was varied in the range {10, 20, 30, 40} mL/min. The dispersed phase flow Q_d was modified accordingly to Q_c, in order to vary the ratio $\Phi = Q_d/Q_c$. For each value of Q_c the tested range of Φ was {0.1, 0.2, 0.4, 0.6, 1, 1.2, 1.5}. This range corresponds to a range of frequency from 2.2 Hz to 121.9 Hz and a range of droplet volume from 4.69 nL to15.7 nL. The same experiment was compared to those acquired in real time imaging of the droplets fluxes using a standard setup (i.e. an inverted microscope coupled with a fast camera) described in [22], by way of comparison.

3. Results and discussions

The aim of this work was to realize an integrated opto-fluidic system for the generation and real-time counting of droplets flowing inside a microfluidic channel, with a system which was more versatile than standard imaging techniques. In this way, the well-known procedure for a microscope trigger can be substituted by fast, reproducible and portable set-up with no need of post-processing data analysis. To achieve

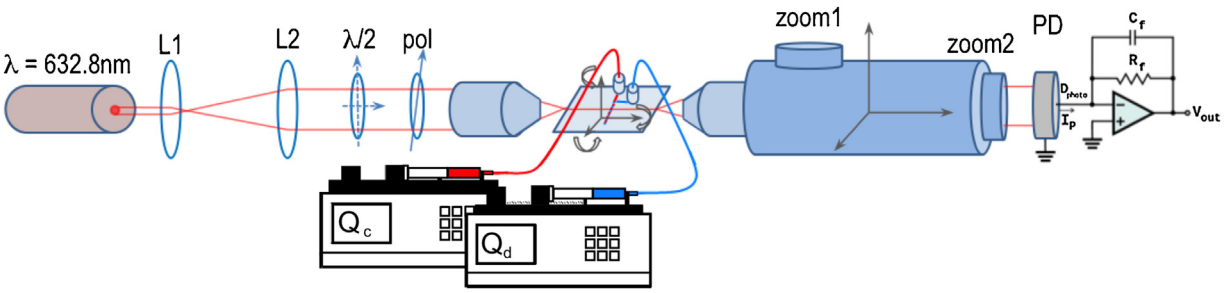

Fig. 2. Experimental setup: a 632.28 nm He-Ne laser was enlarged by two lens (L1,L2) to properly fit the pupil of the objective, then a half wave plate and a polarizer allow the choice of the polarization. The light recollected on the other side of the chip were analyzed by a Vidicon tube in a near field mode. The Vidicon tube was coupled with a 50x objective and were focalized on the external side of the chip. The signal was transduced and amplified into a Voltage value by mean of a photodiode with a transimpedance. The magnification of the whole system is 430x.

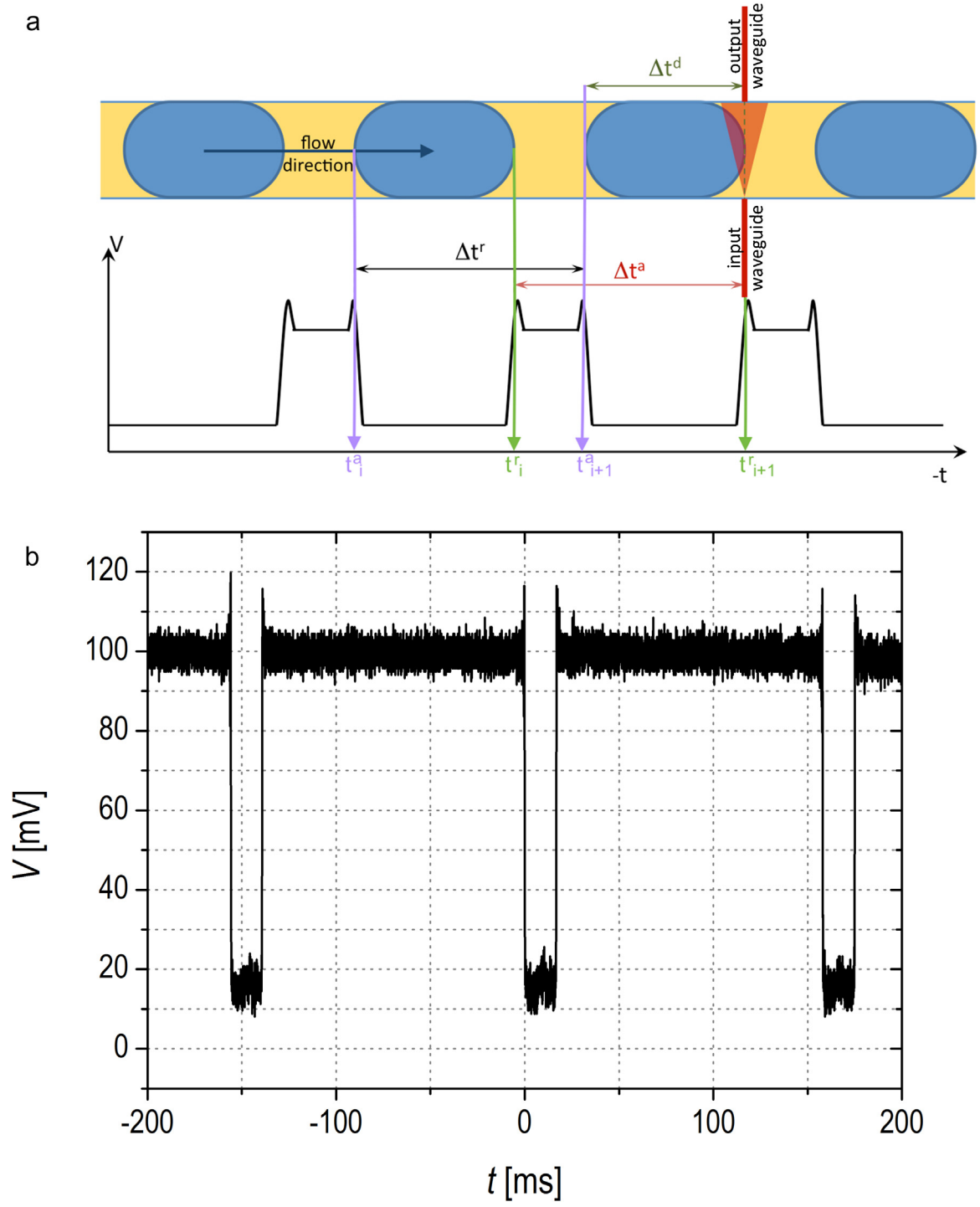

Fig. 3. The working mechanism of the signal: a) Scheme of the time interval measured with the integrated optical trigger system during the passage of droplets, t_i^a (violet) and t_i^r (green) refer respectively to the passage of the receding and advancing menisci. The $\Delta t_d = t^a - t^r$ represents the passage time of a droplet and it's proportional to the droplet length. The $\Delta t_r = t_{i+1}^r - t_i^r$ (black), $\Delta t_a = t_{i+1}^a - t_i^a$ (red) are the duration between the passage of two consecutive menisci, receding and advancing respectively. These parameters are estimators for the period of the droplet generations. b) Example of the voltage signal form the photodiode at the passage of three subsequent droplets. (For interpretation of the references to colour in this figure legend, the reader is referred to the web version of this article.)

this result, the concept was to detect the intensity time dependent signal collected by the output waveguide as an optical trigger.

The working principle of the device is explained in Fig. 3, where the interpretation of a droplets train output signal was sketched (Fig. 3a) and compare with the real output signal (Fig. 3b). Plateaux at different heights alternate, one corresponding to the continuous phase and the other one to the droplet optical transmission detected by the output waveguide. As shown in the sketch in Fig. 3a, the top plateau refers to the flowing of the continuous phase in front of the waveguide, while the bottom one refers to the scattering of light by the droplet surface. In this way, it is possible to measure the time duration Δt_d for the droplet to cross the line of sight of the waveguide. Moreover, system can identify clearly the instant at which advancing and receding menisci flow, since they are detected as "fall" and "rise" of the detected signal, like a droplet trigger. It is worth mentioning that the detected signal contains physical information that are univocally related to the droplet size: (1)

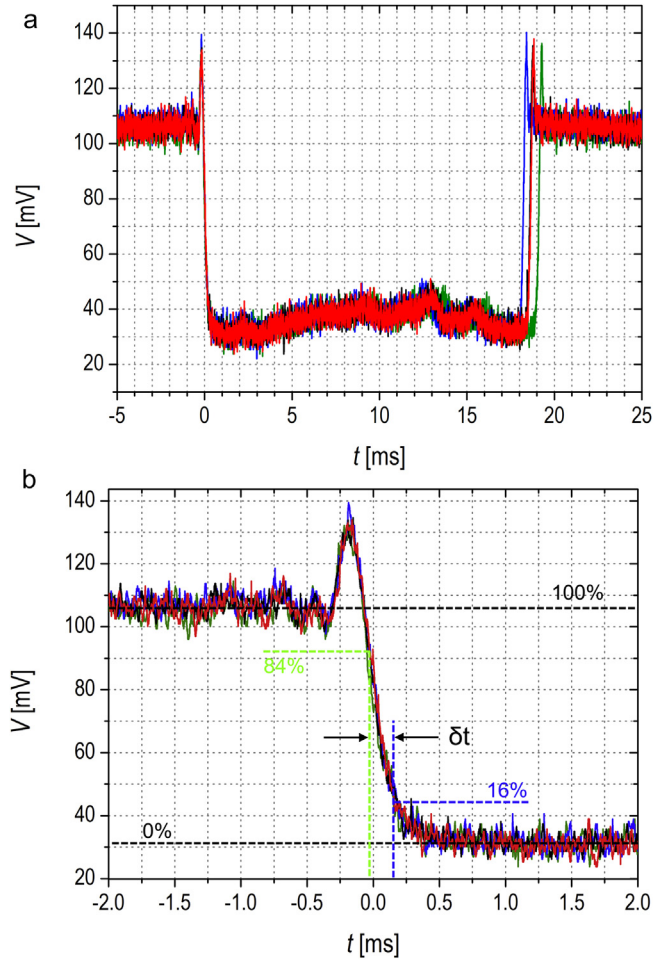

Fig. 4. Reproducibility of the signal and the meniscus: Examples of the superposition of the signal from four different single droplet: a) entire signal of droplets triggered with the fall of the advancing menisci, b) focus on the advancing menisci, where it is also depicted the estimation δt of the uncertainty related to a fall/drop of the signal. Blue lines refer to the 16% of the average fall/drop of the signal, in the same way light green lines refer to the 84%.

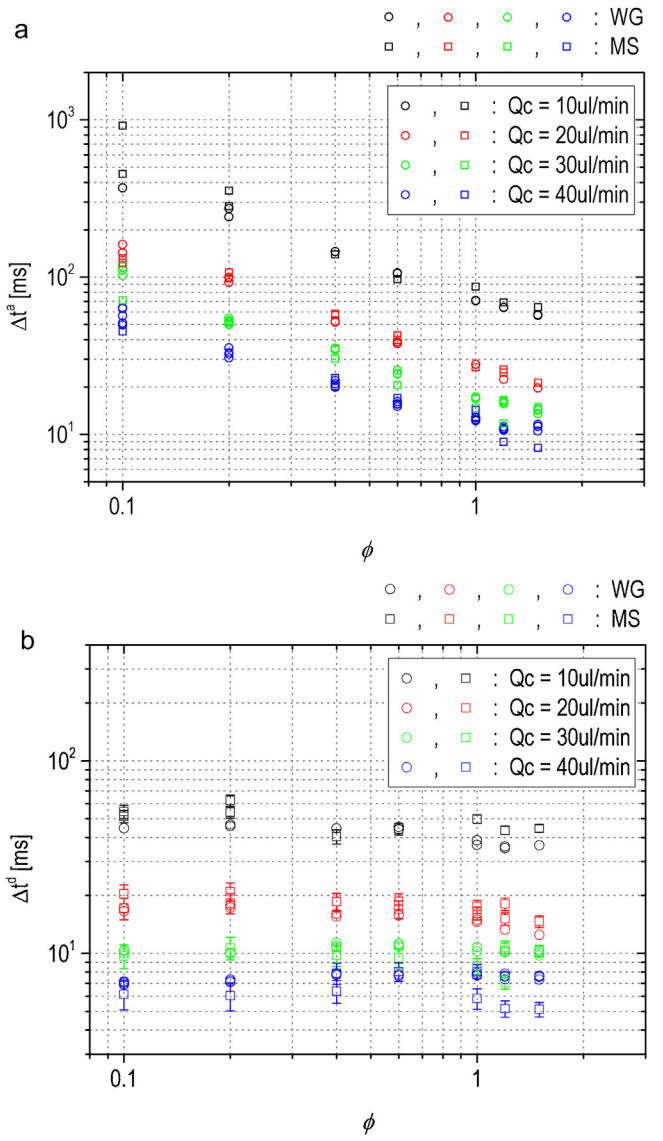

Fig. 5. Comparisons between the microscope setup system (MS) and the droplet measured with the optical trigger system (WG) here presented: a) Δt^a (advancing menisci), b) Δt^d droplet duration (time of passage of a droplets). The Logarithmic scales were set for a better visualization. Error bars were not drawn for the sake of clarity (markers size is bigger than errors). All repeated measurements were reported when available.

the advancing and receding menisci are distinctively identified in the recorded signal, (2) the length of each droplet can be determined without post-imagining techniques; (3) asymmetries in the droplets shape are detected and (4) each single droplet can be individually analyzed. These characteristics make this platform a valid alternative to other set-ups for sensing size and dispersed particle into a fluxed fluid, like capacitive sensor or microscope.

In the following section, we will focus on the study of its performances and potentialities.

3.1. Integrated opto-microfluidics response

The signal period corresponds to the reciprocal of the frequency of droplets generation: Δt^a is the period relative to the advancing menisci whilst Δt^r refers to the receding menisci respectively, as depicted in Fig. 3a. In order to obtain a trigger, the crucial parts of the signal are the rise and the fall due to the passage on the menisci. In all the signals both the rise and fall of the square wave are characterized by defined sharp peaks (Fig. 4a), which identify the interaction behaviors between the light and advancing, receding menisci respectively. Furthermore, these peaks are a fingerprint of the meniscus shape. The droplet curvature along with its refractive index acts as a focusing medium that transiently improve coupling into the output waveguide. Moreover, it is worth mentioning that the rising and falling edges of the detected signal are extremely reproducible (Fig. 4b). The length of the droplet is proportional to droplet duration Δt_d provided that the droplet velocity v is constant. However, It is mandatory to properly define a trustworthy protocol in data analysis to identify the real beginning and the end of each droplet, and the relative error. From the statistical analysis of a large number of droplets trains, it emerged that the best physical quantity representing the beginning (and the end) of a meniscus is the instant t corresponding to the full width at half maximum (FWHM) of the recorded signal, taken with respect to two adjacent plateau (continuous and dispersed phases respectively). A customized software was developed to analyze the detected signal (i.e. the output voltage from the acquisition system) in order to obtain the average signal value of each plateau. The passage time instant t^a of all the advancing menisci was recorded. The difference Δt^a between two subsequent droplets was calculated (see Fig. 5a) as well as its average (Δt^a_{av}) and standard deviation, for each combination of tested flow rates (Q_c = 10, 20, 30, 40 μL/min and for each of this Q_d = 10, 1 {0.1, 0.2, 0.4, 0.6, 1, 1.2, 1.5} Q_c μL/min). The same analyses were performed for the passage times of

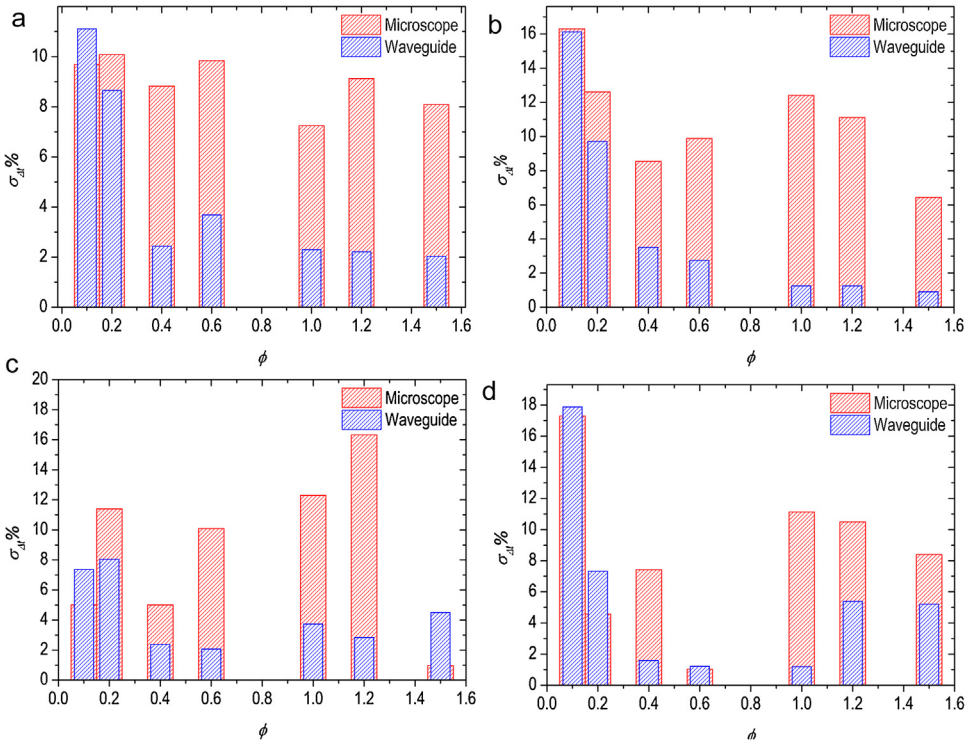

Fig. 6. Comparisons in dispersion between microscope and optical trigger system (WG) here presented: Comparison between the dispersion σ of Δt^a between subsequent droplet obtained with the microscope setup system (red bins) and the droplet measured with the optical trigger system (blue bins), for each tested ϕ and Q_c: a) 10 μL/min, b) 20 μL/min, c) 30 μL/min and d) 40 μL/min. (For interpretation of the references to colour in this figure legend, the reader is referred to the web version of this article.)

the receding menisci Δt^r and of a single droplet Δt^d (see Fig. 5b). The relative difference $(\Delta t^r_{av} - \Delta t^r_{av})/\Delta t^a_{av}$ never exceeded 0.2%, and their dispersion was compatible within 10%. It is worth mentioning that no systematic trends between Δt^a_{av}, Δt^r_{av} across the tested rates was measured, as confirmed also by residuals and covariance tests of cross-linked quantities. In particular the statistical analysis evidenced that there is no distinction in preferring one or the other parameter (Δt^a_{av}, Δt^r_{av}) as an estimator for the droplets frequency.

The uncertainty in the estimation of the time intervals depends on how it is measured the time duration of the rise or fall of the signal. As consequence, a systematic investigation on the precision and accuracy of the measurements was carried out at every experimental configuration previously quoted. The best choice to estimate this time duration in a reproducible way independently of the experimental conditions, was to measure δt between two thresholds fixed at the 16% and 84% of the difference between higher and lower level of plateau, as sketched in Fig. 4b. This estimation depends on the speed and the shape of the droplets, and consequently on the flow rates employed. In this work range, δt was found to vary from 377 ± 4 μs at a flow rates Q_c, Q_d = 10, 1 μL/min down to 50 ± 1 μs at Q_c, Q_d = 40, 60 μL/min. These values are extremely low respect to the time intervals between two droplets. In particular the ratio between δt and Δt^a spreads from 0.4% for first case (Δt^a = 11.21 ± 0.03 ms Q_c, Q_d = 40, 60 μL/min) to 0.1% for the second one (Δt^a = 369 ± 6 ms Q_c, Q_d = 10, 1 μL/min). Moreover, δt results to be very small also compared to the time of passage Δt^d of a single droplet, less than 0.8% for all tested rates.

It is straightforward that an immediate useful application of this integrated opto-microfluidic system is the fast triggering of the droplets in real-time. In microfluidics applications the standard way to measure droplets frequencies and lengths is to employ the experimental setup described in [22], which requires a microscope equipped with fast camera, a data storage and a post-processing software to analyze images. In addition to the bulky setup, the time and the cost of the process is directly proportional to the frequency of the droplets; furthermore, frequency on the order of 1 kHz make a real time processing no more feasible, especially when each single droplet needs to be analyzed separately. On the contrary this configuration has no limit in frequency (as compared to the typical frequency of droplet generator i.e. less than 10 kHz), high portability and low cost, relying on the need of standard and already integrated accessories such as a low power laser, two fibers connected to the microfluidic device and a photodiode with simple electronics triggering a square wave.

3.2. Integrated opto-microfluidics capability

In order to compare the performance of the integrated opto-microfluidic platform and of the standard approaches based on microscope imaging detection, several experiments were performed on trains of 100 droplets at different flow rates. This comparison aimed to evidence the potentialities and possible drawbacks of exploiting a real-time acquisition system that does not use any imaging tool and investigate its use in triggering application.

The comparison between the Δt^a_{av}, Δt^d_{av} (the average over all droplet of Δt^a, Δt^d) obtained by the integrated optical trigger and the time intervals $\Delta t^{a,m}_{av}$, $\Delta t^{d,m}_{av}$ obtained with the microscope imaging in the same conditions are reported in Fig. 5 (the logarithmic scale is just for a better visualization of the data). The results take into account also the uncertainties due to the reproducibility of the measurements made in different laboratories and days. Nevertheless, data from microscope image analysis and from the integrated optical trigger show a good agreement both as single points and as trends (Fig. 5), thus demonstrating the compatibility of the two measurements methods, and the validity of the comparison that is improving at higher ϕ values.

The integrated optical trigger is definitively better than the standard system not only thanks to its fast response time but also due to its higher sensitivity. As a matter of fact, the dispersions of measured Δt (all three parameter considered in the paper) on a population of about 100 droplets were calculated both from the data obtained with the microscope, and from those derived by the optical trigger. The comparison between the two measurement systems is reported in Fig. 6, where the dispersions are plotted for each set value of Q_c at each dispersed flow rate Q_d. If more than one measurement was available, the higher value of the dispersion was plotted. As it can be noted from Fig. 6, apart from few points at the lowest flow rates, the optical trigger

is characterized by a significant lower dispersion in the determination of Δt, in average the optical trigger dispersion is more than 0.5 times of microscope dispersion. In particular, the microscope setup dispersion is constant and does not show any evident trend depending on the microfluidics setup (as evident when looking at the σ dependence on ϕ). While, the optical trigger follows a decreasing trend (lower dispersion at increasing ϕ), demonstrating that it is mainly affected by the natural droplet size dispersion of the generation process. Indeed, the droplet generation fluctuations are expected to decrease with increasing of the flow thanks to the greater system stability. Furthermore, as already stated in [22], this integrated optical-microfluidic platform is able to generate droplets with a size dispersion less than 3% and mono-mode size distribution, which is aligned with standard results obtained in literature with others polymeric substrate [39,40].

4. Conclusion

For the first time, an opto-fluidic platform for droplet generation and optical triggering was completely realized in a single lithium niobate substrate and accurately characterized. The voltage signal output exhibited a high reproducible and stable behavior throughout a wide range of droplet volumes and velocities, and the data follow the same trends observed in microscope-based analysis, but showing less dispersion. Indeed, comparison with the microscope-fast camera method highlighted the good performance of the $LiNbO_3$ device, which reduced the signal reading dispersion of more than 50% respect to the standard setup. Moreover, the droplet signal profile showed how the shape of the voltage signal is directly determined by the droplet size and geometry. So that the beginning and the end of each droplet can be clearly distinguished and associated with the rise and fall of its corresponding electrical signal. These results encourage future applications of $LiNbO_3$-based devices as sensors not only for size and volume of droplet, but also for single particle tracing.

The presence of a fully integrated and self-aligned optical stage, i.e. the waveguides array, will also allow performing a wide range of optical investigations, such as absorption or fluorescence measurements, suitable for deriving physical and chemical properties of droplet. In conclusion, the feasibility of this optofluidic prototype on lithium niobate paves the way for the realization of more complex, independent and portable LOC devices, where the multiple applications of this material in microfluidic and integrated optics fields are exploited.

Acknowledgments

The authors are grateful to the LaFSI (Laboratorio di fisica delle superfici e interfacce) group of the Physics and Astronomy Department of Padova for the useful discussions about microfluidics. Special thanks are due to Enrico Chiarello for providing the image analysis software. Finally, the authors gratefully acknowledge financial support of the University of Padova, funding the project BIRD165523/16: “Biosensing Light-Driven Tools in Advanced Opto-Microfluidic Lithium Niobate Platform” and the Ca.Ri.Pa.Ro foundation in the framework of the Excellence Project “Integrated Opto-Microfluidic Prototype on Lithium Niobate Crystals for Sensing Applications” (call 2011–2012). This work was also partly supported by the French RENATECH network and its FEMTO-ST MIMENTO technological facility.

References

[1] G.M. Whitesides, The origins and the future of microfluidics, Nature 442 (2006) 368–373.
[2] N.T. Nguyen, S. Lassemono, F.A. Chollet, Optical detection for droplet size control in microfluidic droplet-based analysis systems, Sens. Actuators B: Chem. 117 (2006) 431–436, https://doi.org/10.1016/j.snb.2005.12.010.
[3] Y.W. Hsieh, A.B. Wang, X.Y. Lu, L.A. Wang, High-throughput on-line multi-detection for refractive index, velocity, size, and concentration measurements of micro-two-phase flow using optical microfibers, Sens. Actuators B: Chem. 237 (2016) 841–848, https://doi.org/10.1016/j.snb.2016.07.027.
[4] C. Kunstmann-Olsen, M.M. Hanczyc, J. Hoyland, S. Rasmussen, H.G. Rubahn, Uniform droplet splitting and detection using Lab-on-Chip flow cytometry on a microfluidic PDMS device, Sens. Actuators B: Chem. 229 (2016) 7–13, https://doi.org/10.1016/j.snb.2016.01.120.
[5] P.K. Shivhare, A. Prabhakar, A.K. Sen, Optofluidics based lab-on-chip device for in situ measurement of mean droplet size and droplet size distribution of an emulsion, J. Micromech. Microeng. 27 (2017), https://doi.org/10.1088/1361-6439/aa53cc.
[6] E. Weber, M.J. Vellekoop, Optofluidic micro-sensors for the determination of liquid concentrations, Lab Chip 12 (2012) 3754, https://doi.org/10.1039/c2lc40616k.
[7] L. Novak, P. Neuzil, J. Pipper, Y. Zhang, S. Lee, An integrated fluorescence detection system for lab-on-a-chip applications, Lab Chip 7 (2007) 27–29, https://doi.org/10.1039/B611745G.
[8] S.U. Hassan, A.M. Nightingale, X. Niu, Optical flow cell for measuring size, velocity and composition of flowing droplets, Micromachines 8 (2017), https://doi.org/10.3390/mi8020058.
[9] M.R. De Saint Vincent, S. Cassagnére, J. Plantard, J.P. Delville, Real-time droplet caliper for digital microfluidics, Microfluid. Nanofluid. 13 (2012) 261–271, https://doi.org/10.1007/s10404-012-0955-1.
[10] J.Z. Chen, A.A. Darhuber, S.M. Troian, S. Wagner, Capacitive sensing of droplets for microfluidic devices based on thermocapillary actuation, Lab Chip 4 (2004) 473, https://doi.org/10.1039/b315815b.
[11] C. Elbuken, T. Glawdel, D. Chan, C.L. Ren, Detection of microdroplet size and speed using capacitive sensors, Sens. Actuators A: Phys. 171 (2011) 55–62, https://doi.org/10.1016/j.sna.2011.07.007.
[12] P. Kubra Isgor, M. Marcali, M. Keser, C. Elbuken, Microfluidic droplet content detection using integrated capacitive sensors, Sens. Actuators B: Chem. 210 (2015) 669–675, https://doi.org/10.1016/j.snb.2015.01.018.
[13] X. Niu, M. Zhang, S. Peng, W. Wen, P. Sheng, Real-time detection, control, and sorting of microfluidic droplets, Biomicrofluidics 1 (2007), https://doi.org/10.1063/1.2795392.
[14] E.V. Moiseeva, A.A. Fletcher, C.K. Harnett, Thin-film electrode based droplet detection for microfluidic systems, Sens. Actuators B: Chem. 155 (2011) 408–414, https://doi.org/10.1016/j.snb.2010.11.028.
[15] B. Bhattacharjee, H. Najjaran, Droplet sensing by measuring the capacitance between coplanar electrodes in a digital microfluidic system, Lab Chip 12 (2012) 4416, https://doi.org/10.1039/c2lc40647k.
[16] N. Yi, B.K. Park, D. Kim, J. Park, Micro-droplet detection and characterization using thermal responses, Lab Chip 11 (2011) 2378, https://doi.org/10.1039/c0lc00728e.
[17] P. Friis, K. Hoppe, O. Leistiko, K.B. Mogensen, J. Hübner, J.P. Kutter, Monolithic integration of microfluidic channels and optical waveguides in silica on silicon, Appl. Opt. 40 (2001) 6246, https://doi.org/10.1364/AO.40.006246.
[18] K.B. Mogensen, J. El-Ali, A. Wolff, J.P. Kutter, Integration of polymer waveguides for optical detection in microfabricated chemical analysis systems, Appl. Opt. 42 (2003) 4072, https://doi.org/10.1364/AO.42.004072.
[19] R. Osellame, V. Maselli, R.M. Vazquez, R. Ramponi, G. Cerullo, Integration of optical waveguides and microfluidic channels both fabricated by femtosecond laser irradiation, Appl. Phys. Lett. 90 (2007), https://doi.org/10.1063/1.2747194.
[20] G. Pozza, S. Kroesen, G. Bettella, A. Zaltron, M. Esseling, G. Mistura, P. Sartori, E. Chiarello, M. Pierno, C. Denz, C. Sada, T-junction droplet generator realised in lithium niobate crystals by laser ablation, Optofluid. Microfluid. Nanofluid. 1 (2014), https://doi.org/10.2478/optof-2014-0003.
[21] A. Zaltron, G. Bettella, G. Pozza, R. Zamboni, M. Ciampolillo, N. Argiolas, C. Sada, S. Kroesen, M. Esseling, C. Denz, Integrated optics on lithium niobate for sensing applications, SPIE Opt. Optoelectron. (2015) 950608, https://doi.org/10.1117/12.2178457.
[22] G. Bettella, G. Pozza, S. Kroesen, R. Zamboni, E. Baggio, C. Montevecchi, A. Zaltron, L. Gauthier-Manuel, G. Mistura, C. Furlan, M. Chauvet, C. Denz, C. Sada, Lithium niobate micromachining for the fabrication of microfluidic droplet generators, Micromachines 8 (2017), https://doi.org/10.3390/mi8060185.
[23] M. Chauvet, F. Henrot, F. Bassignot, F. Devaux, L. Gauthier-Manuel, V. Pecheur, H. Maillotte, B. Dahmani, High efficiency frequency doubling in fully diced $LiNbO_3$ ridge waveguides on silicon, J. Opt. (United Kingdom) 18 (2016), https://doi.org/10.1088/2040-8978/18/8/085503.
[24] W. Sohler, H. Hu, R. Ricken, V. Quiring, C. Vannahme, H. Herrmann, D. Büchter, S. Reza, W. Grundkötter, S. Orlov, others Integrated optical devices in lithium niobate, Opt. Photon. News 19 (2008) 24–31.
[25] M. Bazzan, C. Sada, Optical waveguides in lithium niobate: recent developments and applications, Appl. Phys. Rev. (2015) 2.
[26] J. Friend, L.Y. Yeo, Microscale acoustofluidics: microfluidics driven via acoustics and ultrasonics, Rev. Mod. Phys. 83 (2011) 647–704, https://doi.org/10.1103/RevModPhys.83.647.
[27] M. Jubera, García-Cabañes, J. a Olivares, Alcazar, M. a Carrascosa, Particle trapping and structuring on the surface of $LiNbO_3$:Fe optical waveguides using photovoltaic fields, Opt. Lett. 39 (2014) 649–652, https://doi.org/10.1364/OL.39.000649.
[28] M. Esseling, A. Zaltron, W. Horn, C. Denz, Optofluidic droplet router, Laser Photon. Rev. 9 (2015) 98–104, https://doi.org/10.1002/lpor.201400133.
[29] B. Fan, F. Li, L. Chen, L. Shi, W. Yan, Y. Zhang, S. Li, X. Wang, X. Wang, H. Chen, Photovoltaic manipulation of water microdroplets on a hydrophobic $LiNbO_3$ substrate, Phys. Rev. Appl. 7 (2017), https://doi.org/10.1103/PhysRevApplied.7.064010.
[30] M. Gazzetto, G. Nava, A. Zaltron, I. Cristiani, C. Sada, P. Minzioni, Numerical and experimental study of optoelectronic trapping on iron-doped lithium niobate substrate, Crystals 6 (2016) 123, https://doi.org/10.3390/cryst6100123.
[31] L. Lucchetti, K. Kushnir, A. Zaltron, F. Simoni, Light controlled phase shifter for optofluidics, Opt. Lett. 41 (2016) 333–335, https://doi.org/10.1364/OL.41.

000333.
[32] M. Chauvet, L. Al Fares, B. Guichardaz, F. Devaux, S. Ballandras, Integrated opto-fluidic index sensor based on self-trapped beams in $LiNbO_3$, Appl. Phys. Lett. (2012) 101.
[33] G. Pozza, S. Kroesen, G. Bettella, A. Zaltron, M. Esseling, G. Mistura, P. Sartori, E. Chiarello, M. Pierno, C. Denz, others T-junction droplet generator realised in lithium niobate crystals by laser ablation, Optofluid. Microfluid. Nanofluid. (2014) 1.
[34] R. Osellame, Femtosecond-laser-based microstructuring and modification of transparent materials, Adv. Solid State Lasers (2015) AF1A-1.
[35] D. Huo, Z.J. Choong, Y. Shi, J. Hedley, Y. Zhao, Diamond micro-milling of lithium niobate for sensing applications, J. Micromech. Microeng. 26 (2016), https://doi.org/10.1088/0960-1317/26/9/095005.
[36] E.L. Wooten, K.M. Kissa, A. Yi-Yan, E.J. Murphy, D.A. Lafaw, P.F. Hallemeier, D. Maack, D.V. Attanasio, D.J. Fritz, G.J. McBrien, D.E. Bossi, Review of lithium niobate modulators for fiber-optic communications systems, IEEE J. Sel. Top. Quantum Electron. 6 (2000) 69–82, https://doi.org/10.1109/2944.826874.
[37] S.M. Langelier, L.Y. Yeo, J. Friend, UV epoxy bonding for enhanced SAW transmission and microscale acoustofluidic integration, Lab Chip 12 (2012) 2970, https://doi.org/10.1039/c2lc40085e.
[38] J. Bennès, S. Ballandras, F. Chérioux, Easy and versatile functionalization of lithium niobate wafers by hydrophobic trichlorosilanes, Appl. Surf. Sci. 255 (2008) 1796–1800, https://doi.org/10.1016/j.apsusc.2008.06.031.
[39] G.F. Christopher, N.N. Noharuddin, J.A. Taylor, S.L. Anna, Experimental observations of the squeezing-to-dripping transition in T-shaped microfluidic junctions, Phys. Rev. E – Stat. Nonlinear, Soft Matter Phys. 78 (2008) 1–12, https://doi.org/10.1103/PhysRevE.78.036317.
[40] E. Piccin, D. Ferraro, P. Sartori, E. Chiarello, M. Pierno, G. Mistura, Generation of water-in-oil and oil-in-water microdroplets in polyester–toner microfluidic devices, Sens. Actuators B: Chem. 196 (2014) 525–531, https://doi.org/10.1016/j.snb.2014.02.042.

Bettella Giacomo PhD in physics, he is expert in optics, waveguides, microfluidics and thin film deposition. As a postdoctoral fellow at the Physics and Astronomy Department of the University of Padova he has been involved in a research project on the realization of portable microfluidic devices for optical sensing of water solutions.

Riccardo Zamboni Master in Physics, he is PhD student at the University of Padova. He is expert in opto-microfluidics and integrated optics for applications in optical sensing, and optical and microfluidics platform development.

Pozza Gianluca PhD in Material Science, he focused on the fabrication of optofluidic platforms integrated in lithium niobate for sensing applications. In particular he focused on the fabrication and characterization of optical devices (Ti in-diffused waveguides, PPLN structures for SHG) and to the realization and characterization of microfluidic channels engraved in lithium niobate. He was involved in the development of a SPR-based biosensing platform for the detection of L. pneumophila bacteria.

Zaltron Annamaria took the PhD in physics is a Researcher at the Department of Physics and Astronomy of the University of Padova. Her research activity concerns the characterization and optimization of the optical and structural properties of lithium niobate crystals in order to realize integrated optical devices and opto-fluidic platforms for sensing applications in different research areas. Moreover, recently she has started to study and exploit the photovoltaic properties of this material to actuate on particles, droplets and liquid crystals inside integrated opto-microfluidic circuits.

Carlo Montevecchi Master in Physics, he is PhD student at the Quantum Photonics Laboratory at Heriot Watt University working in the field of integrated optics and microfluidic characterization.

Pierno Matteo Associate Professor at the Department of Physics and Astronomy 'Galileo Galilei' of the University of Padua, his research interests are focused on complex fluids, liquids at interfaces and oscillators as probes of nanofriction and energy dissipation at the microscopic level in atomistic mono- and multi-layers. Along his investigations light scattering and optical microscopy techniques have been extensively used. The addressed specific topics may be grouped in two main areas: (i) the study of the structural properties, the microscopic dynamics, and the phase transitions in soft condensed matter systems, and (ii) surface and interfaces properties of liquid/liquid/solid/liquid and gas/solid interfaces.

Giampaolo Mistura received his MS degree in physics from Padua University (Italy) in 1986. He obtained his PhD degree from Penn State University (USA) in 1993, working on the wetting properties of cryogenic fluids. He spent 1 year at the University of Konstanz (Germany) and one at the High Magnetic Field Laboratory in Grenoble (France). Since 1994 he is at the Physics Department of Padua University (Italy) where he is currently associate professor. His main research activities include the study of interfacial phenomena (wetting and nanofriction) and microfluidics.

Sada Cinzia born in 1973, she is Associate Professor in Physics at the Department of Physics and Astronomy of the University of Padova. Her main research topics concern the development of lithium niobate platforms for applications in integrated optics, optical sensing and opto-microfluidics, film coating for sensing applications and the study of materials and processes for the tailored modification of surfaces and interfaces response. She is coauthor of more than 250 publications in international peer-reviewed journals, (h-index is 38).

Gauthier-Manuel Ludovic Expert in optics, micromachining and microfluidics he is working as researcher at the Institut FEMTO-ST | FEMTO ST, Department of Optics, University of Franche-Comté in Besançon.

Chauvet Mathieu was born in Vannes, France, on June 13, 1967. He graduated from the national engineering school in Brest (E.N.I.Br.) in 1990 and earned a Ph.D. in electronics from university of Brest in 1994. His doctoral work was carried out at France Telecom graduate engineering school in Brittany (ENST) on nonlinear semiconductor photorefractive waveguides applied to optical telecommunications. He is currently working as a professor at university of Franche-Comté in Besançon (France) where he is engaged in research on spatial solitons using photorefractive effects.